Since January 2020 Elsevier has created a COVID-19 resource centre with free information in English and Mandarin on the novel coronavirus COVID-19. The COVID-19 resource centre is hosted on Elsevier Connect, the company's public news and information website.

Energy and Buildings 55 (2012) 118–126

Contents lists available at SciVerse ScienceDirect

Energy and Buildings

journal homepage: www.elsevier.com/locate/enbuild

A preference driven multi-criteria optimization tool for HVAC design and operation

Jovan Pantelic*, Benny Raphael, Kwok Wai Tham

Department of Building, School of Design and Environment, National University of Singapore, 4 Architecture Drive, 117566 Singapore, Singapore

ARTICLE INFO

Article history:
Received 9 November 2011
Received in revised form 12 April 2012
Accepted 21 April 2012

Keywords:
Multi-criteria optimization
Airborne infection risk
Energy
Thermal comfort
Personalized ventilation
Mixing ventilation

ABSTRACT

This paper discusses the issue of selecting the design solution that best accords with an articulated preference of multiple criteria with an acceptable performance band. The application of a newly developed multi-criteria decision-making tool called RR-PARETO2 is presented. An example of HVAC design is used to illustrate how solutions could be selected within a multi-criteria optimization framework. In this example, five criteria have been selected, namely, power consumption, thermal comfort, risk of airborne infection of influenza and tuberculosis and effective differential temperature (Δt_{eq}) of body parts. The goal is to select the optimal air exchange rate that makes reasonable trade-offs among all the objectives. Two scenarios have been studied. In the first scenario, there is an influenza outbreak and the important objective is to prevent the spread of infection. In the second scenario, energy prices are high and the primary objective is to reduce energy. In both scenarios, RR-PARETO2 algorithm selects solutions that make reasonable trade-offs among conflicting objectives. The example illustrates how objectives such as reduction of airborne disease transmission and maximizing thermal comfort can be incorporated in the design of a practical, full-scale HVAC system.

1. Introduction

Optimization techniques are increasingly being used for the design of building systems. Huh and Brandemuehl [1] optimized HVAC system performance using five systems variables to minimize energy consumption while meeting building loads and maintaining thermal comfort. Wemhoff [2] used multi-dimensional interpolation between optimized control configurations for several steady-state load distributions to reduce energy consumption of an HVAC system. Other examples can be found in [3–5]. Realizing the importance of optimization of building systems, some simulation softwares such as Ecotect [6] already provide options for design optimization.

The development of direct search methods [7] has contributed to the use of optimization in design. These techniques use the concept of black box optimization in which the objective function need not have an explicit mathematical representation. The objective function might involve executing external programs which are treated as black-boxes by the optimization algorithm. Unlike traditional mathematical optimization, mathematical characteristics of the evaluation function including convexity, expression for the gradient, etc. are not needed. Examples of direct search methods include Genetic Algorithms [8], Simulated Annealing [9] and PGSL [10]. These algorithms make it possible to minimize objective functions such as energy which require running simulations as external programs.

While minimizing the energy consumption of HVAC system has been the primary goal of several building related optimization studies, recent studies have highlighted the importance of other factors. After the emergence of Severe Acute Respiratory Syndrome (SARS) in 2003 and the resurgence of Influenza in 2009, airborne infection transmission became one of the most important concerns in densely occupied indoor environments. HVAC system has a large impact on airborne transmission [11,12]. Hence reduction of airborne disease transmission is a very important consideration that has to be taken into account besides minimizing energy consumption. Optimization of HVAC systems using this criterion has not been attempted so far.

When factors such as disease transmission are considered along with energy consumption, design becomes a multi-objective optimization problem. The multi-objective approach to design optimization has been applied by several researchers. Wright et al. [13] investigated application of a multi-objective genetic algorithm to find pay-off characteristic between the energy cost of a building and the occupant thermal comfort. Djuric et al. [14] performed optimization of HVAC system based on energy consumption, investment cost and thermal comfort using generic

* Corresponding author. Tel.: +65 81188207.
E-mail addresses: bdgjp@nus.edu.sg (J. Pantelic), bdgbr@nus.edu.sg (B. Raphael), bdgtkw@nus.edu.sg (K.W. Tham).

0378-7788/$ – see front matter © 2012 Elsevier B.V. All rights reserved.
http://dx.doi.org/10.1016/j.enbuild.2012.04.021

optimization program. Hamdy et al. [15] used multi objective genetic algorithm to optimize HVAC system performance for primary energy conservation. However, the decision-making process involving multiple criteria is still not well established. For example, a building design that maximises natural day lighting may not perform well with respect to the total energy consumption, since it might have high cooling loads in tropical climates. Decision-making in such situations is not straightforward because trade-offs have to be made between user's preference for natural day lighting and the goal of reducing energy consumption.

This paper discusses the issue of evaluating design alternatives according to multiple criteria and selecting the solution that best accords with user defined preferences and performance bands in a design process. A recently developed algorithm called RR-PARETO2 is applied to the design of an air distribution system in order to illustrate the concept of multi-criteria decision-making. The decision variable is the air exchange rate (ACH). Five criteria have been selected, namely, power consumption, thermal comfort, risk of infection of influenza and tuberculosis and manikin based equivalent temperature difference of the facial region (Δt_{eq}). The goal is to select the optimal ACH that makes reasonable trade-offs among all the objectives. The example illustrates how these objectives are computed in a practical, full-scale air delivery system, and how a design decision is made through multi-criteria optimization.

2. Methodology and experimental design

2.1. Multi-criteria optimization

Currently, single objective optimization is used in most design applications (for example see [3–5]). However, complex engineering artefacts such as building systems have to be necessarily evaluated according to multiple criteria. The task of selecting the best design is complex since it involves making trade-offs among conflicting objectives. Rarely, we find solutions that perform equally well with respect to all the criteria. One approach for accommodating multiple criteria in evaluation is the use of weight factors to combine the effects of all the criteria into a single utility function. A variation of this is presented in [16], in which a multiplicative utility function is used and the weights are determined through an opinion based survey conducted on experts in the domain. The difficulties with this approach are the subjectivity of the importance factors and the efforts required to obtain a reasonable survey sample to improve the accuracy of assessment. Several other methods for multi-criteria decision-making involving the use of weight factors are summarized in [16–18].

Another approach to managing multiple criteria is Pareto optimization in which a population of solutions that are non-dominated is generated. Such techniques have already been used in the design of building systems. For example, Jelle and Arnold [19] used genetic algorithms to find and select Pareto optimal solutions for the trade-off between energy and the risk of exposure to pollutants. However, they do not present a well-defined algorithm for selecting a single solution from the Pareto front. Instead, it is recommended that the practical selection of system configuration should be limited to the midrange spectrum of the Pareto front, where the curvature is the maximum. In fact, researchers have not paid much attention to the problem of selecting the best solution from the Pareto set. In many applications, the final selection of the solution is usually left to the designer (for example see [20,21]).

This work uses a recently developed algorithm called RR-PARETO2 [22,23] that aims to select a single solution with the best trade-offs within a multi-objective framework. In this algorithm, the solution with the best trade-offs among all the objectives is chosen using two pieces of information, ranking of the objectives according to their importance; and the sensitivity of each objective.

The sensitivity of an objective refers to the threshold which determines whether the differences in the objective function values are significant. All the points lying within the specified sensitivity band are considered to be equivalent with respect to that objective. In order to illustrate the concept of sensitivity, consider the objective of minimizing the power consumption. The user might specify that reduction in power below 10% is not significant, and therefore, the sensitivity of this objective is defined as 10%. All the solutions lying within the sensitivity band are considered to be equivalent. These solutions are further filtered using other objectives.

The algorithm starts off with a set of solutions that are generated by any optimization process (Fig. 1). Each solution point contains the values for all the objectives as well as decision variables (optimization variables). The set of solutions are sequentially filtered according to the order of importance of objectives. Filtering is done in two stages. In the first stage, the solution point with the best value for the current objective is chosen from among all the points. All the points that lie outside the sensitivity band of the chosen point are eliminated from the set. If the sensitivity is not specified for any objective, no filtering is done for this objective and all the solutions are retained. At the end of Stage 1, one or more points might remain in the solution set. If a unique solution is not identified, Stage 2 filtering is performed.

In Stage 2 filtering, the hypercube containing all the remaining solutions is trimmed. This is done by dividing the hypercube volume into half by bisecting each objective axis one by one according to their order of importance. Let $ymin_i$ and $ymax_i$ be the minimum and maximum values of the ith objective among all the solutions in the current set. The threshold is computed as $(ymin_i + ymax_i)/2$. In the minimization problem, all the solutions that have a value greater than this threshold are removed from the set. After completing all the objectives, the process is repeated starting from the first objective. The process stops when a single solution remains in the set or all the remaining solutions have the same values for all the objective functions.

Within each iteration of Stage 2 filtering, the inferior half of the solution space according to a criterion is eliminated as shown in Fig. 2. The area **V1** contains solutions with high values of the first objective and this is eliminated in the first iteration. From among remaining solutions, the inferior half of the space **V2** according to the second objective is identified. The solutions that lie within **V2** are then eliminated and the process is repeated until a single solution remains in the set. It should be noted that this process need not necessarily eliminate exactly half the number of solutions in each iteration, since the inferior half of the hypercube might contain fewer solutions. The iterative process is aimed at removing relatively high values at each stage, irrespective of how the points are clustered within the space. By repeating this process for each objective, each criterion is given an opportunity to eliminate inferior solutions and the final selection is a trade-off among all the objectives. It is further emphasized that the process does not favour the best solution according to any objective. For example, if the best solution according to the first objective lies within the inferior half of the second objective, this solution is eliminated. A solution with a better trade-off is one which lies within the better half of the first objective as well as the better half of the second objective. Since the process is driven by the order of importance of objectives, the users' preferences in the selection process are also respected.

An interactive process with good computer support for decision-making is proposed for the selection of the most attractive solution according to multiple criteria. Appropriate visualization of the solution space allows designers to appreciate the range of possibilities and judge the trade-offs that need to be made. It helps them define the sensitivities of objectives by visually evaluating what might

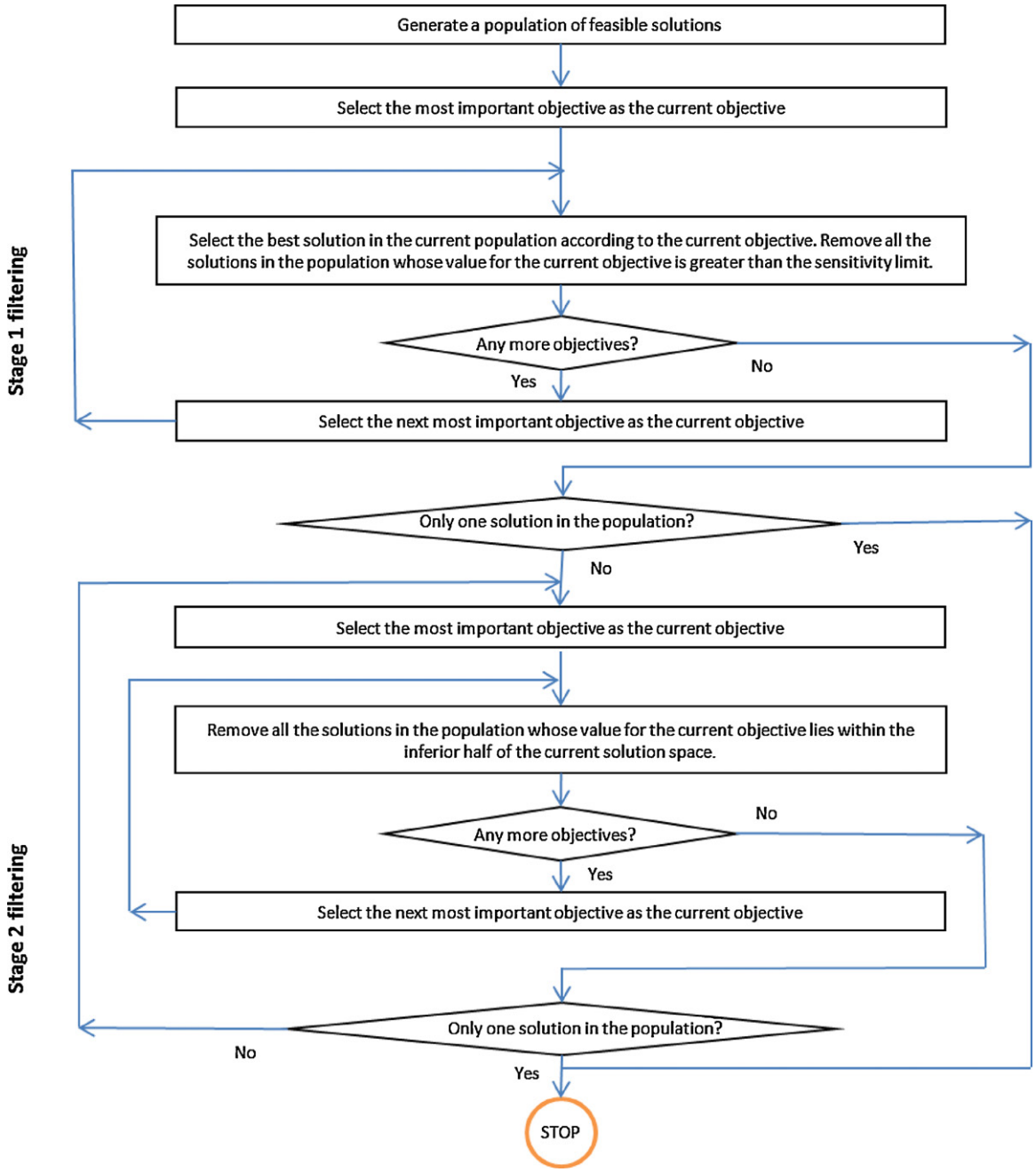

Fig. 1. Flow chart for RR-PARETO2 filtering.

be acceptable increases in objective function values. If users find certain parts of the solution space unattractive they can eliminate these regions through the user interface. On the other hand, if they prefer certain ranges of values of parameter values, they can preselect these regions and the automatic filtering algorithm is applied only after the manual filtering done by the designers. Since the process is simple and fast, designers can attempt many trials, and make the final selection after studying the effects of his preferences.

A graphical user interface (GUI) was developed to help users explore the solution space and perform the selection of the most attractive solution. The GUI uses parallel axis plot for visualizing the values of variables. In a parallel axis plot, the values of variables are plotted along vertical axes and each solution point is represented as a curve connecting points on these axes. This form of plotting permits visualizing a large number of attributes at the same time, which is not easy with conventional 3D and 2D plots. Users can evaluate various possibilities by setting constraints on the values of variables through selecting continuous regions along each axis. In addition, the newly developed RR-PARETO2 filtering can be applied for automatic selection of solution points.

2.2. Instruments

A Field Environmental Chamber (FEC) with the dimensions 11.1 m × 8 m × 2.6 m was used as the experimental facility in this study. The air in the FEC was supplied from an Air Handling Unit (AHU) using ceiling mounted mixing ventilation (MV) air delivery system. The second air delivery system used is a hybrid system consisting of desktop personalized ventilation (DPV) coupled with MV. Personalized ventilation is a recent innovation designed to deliver

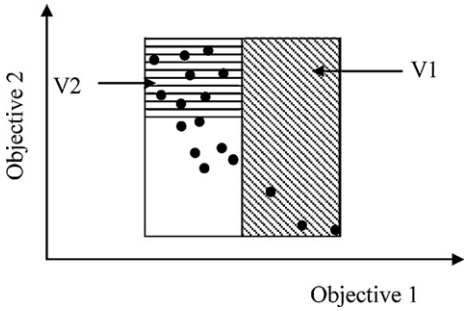

Fig. 2. Trimming of hypercube volume.

clean and conditioned outdoor air directly to the breathing zone of occupants and has been demonstrated to be energy efficient as well as effective in mitigating airborne transmission of infectious expiratory droplets [24]. Independent outdoor air AHU was used to supply air to the DPV.

A cough machine was used to simulate multiphase flow consisting of expiratory droplets suspended in the air released by human cough. Human saliva was simulated with a mixture of water (94% of the total volume) and glycerin (6% of the total volume). This method of human saliva simulation has been used in several studies [24–26]. Further details can be found in [24].

Simulation of a susceptible person in an office environment was achieved using a seated breathing thermal manikin (BTM). The BTM was dressed to approximately 0.7 clo, typical office attire in the tropics. The 26 body segments of the BTM were heated and individually controlled to simulate heat rejection of a human body. To simulate breathing under light office work, the pulmonary ventilation volume was set at 6 l/min, with a 10 times per minute breathing cycle comprising 2.5 s inhalation, 1.0 s break, 2.5 s exhalation and 1.0 s break again, similar to that adopted by Zhu et al. [27].

In order to obtain the concentration time profile of the simulated expiratory aerosols, aerosol counting is required. A Grimm 1.108 aerosol spectrometer with 16 size channels (measurable size range, 0.3–20 μm) was used to measure the real-time aerosol concentration in the inhalation zone of the breathing thermal manikin.

An INNOVA 1312 photoacoustic spectrometer multi-gas analyzer was used to determine air exchange rate (ACH) in the FEC using tracer decay method by measuring the concentrations of sulphur hexafloride over time [28].

2.3. Experimental design

Experiments were designed to simulate susceptible occupant in the office environment supplied with ceiling mounted MV and hybrid system consisting of MV and DPV. The BTM was positioned at the center of FEC sitting at the office table. Air was supplied at the flow rates of 0 (no air supply), 3, 6, 9 and 12 ACH to simulate various operating conditions. Airborne infection risk was also estimated when air was not supplied to the FEC (0 ACH) to simulate condition of possible system failure. Changes of the supply flow rate represented as air exchange rates in FEC results in different energy consumption of the HVAC system, thermal comfort of the occupants and airborne infection risk levels. Droplet concentration in the breathing zone of the BTM was measured with Grimm 1.108 aerosol spectrometer with isokinetic sampling probe positioned 15 mm vertically below the manikin's nose and 15 mm horizontally from the BTM's upper lip. Release of potentially infectious cough droplets was simulated for sitting and standing postures (1.15 m and 1.5 m from the floor, respectively) of the infected occupant while BTM was kept in the seated posture to simulate susceptible occupant performing desk tasks at the designated workplace, while infector was assumed to release cough droplets while sitting or walking (standing posture). Cough was injected at four distances, eight positions along each distance and eight relative orientations between source and receiver for each position. Further details of the experimental design can be found in [29].

The air temperature in the FEC was maintained at 23 °C in all the experimental runs. DPV consisted of 100% outdoor air (OA) with a total flow rate of 5 l/s (2.5 l/s for each ATD) at a temperature of 23 °C. The relative humidity in the room was maintained below 70%.

2.4. Thermal comfort evaluation

Thermal comfort at various conditions for MV has been evaluated using the method proposed by Tanabe et al. [30]. BTM was used to measure the mean skin temperature under thermal neutrality for 26 body segments. Mean skin temperature (t_s) was used to calculate manikin based equivalent temperature for every BTM body segment. Manikin based equivalent temperature (t_{eq}) is defined as: "the temperature of a uniform enclosure in which a thermal manikin with realistic skin surface temperatures would lose heat at the same rate as it would in the actual environment". Value of manikin based equivalent temperature was used as air and radiant temperature for calculation of predicted mean vote (PMV) and percentage of people dissatisfied (PPD) [31]. Other ambient parameters used for this calculation were air velocity of 0 m/s, relative humidity 60% while metabolic rate used was 1.1 met and 0.7 clo for clothing level.

When hybrid DPV system was used, predicting thermal comfort of occupants solely based on the Δt_{eq} is not correct because local air movement in the facial region causes increase of forced convection heat transfer while rest of the body was exposed to dominantly natural convective heat transfer. This can cause thermal asymmetry since facial cooling is significantly higher than the rest of the body. Thermal asymmetry can further lead to thermal discomfort and can be indicated by facial region manikin based equivalent temperature difference (Δt_{eq}). This criterion was added to the overall thermal body sensation to evaluate thermal performance of hybrid DPV system. This additional criterion is very important parameter because DPV supply temperature and flow rate are more critical than ambient temperature for occupant's thermal comfort [32].

2.5. Energy consumption evaluation

Total energy consumption of the HVAC was divided into two parts: (i) transportation and (ii) cooling load. Transportation energy consumption was calculated using Bernoulli's equation taking into account frictional and local losses due to changes of the ductwork geometry in the supply and return system. Geometry of the FEC was modeled in Energy Plus and thermal properties of walls, floor, ceiling and windows, lighting features, occupancy, additional internal heat sources were set in the software for the cooling load calculation. Cooling load calculations were then used to calculate energy consumed by the chiller in order to meet required thermal load.

2.6. Airborne infection risk evaluation

Cough droplets concentration in the breathing zone of the BTM was measured at supply flow rate of 0, 3, 6, 9 and 12 ACH. Results were then averaged using methodology described in [29] which takes into account various distances, positions, postures and orientations between source and receiver and contribution of different air patterns generated in the indoor environment with the air delivery system.

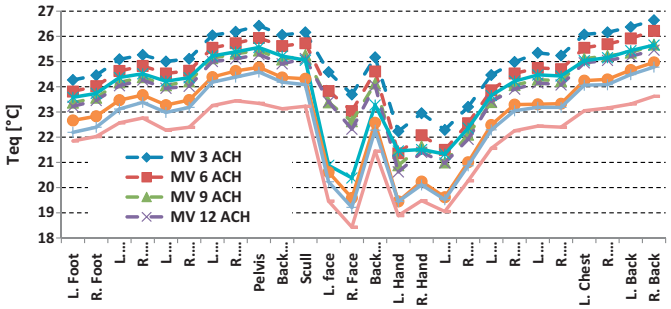

Fig. 3. Manikin based equivalent temperatures for different body parts for MV and DPV.

3. Results and discussion

3.1. Thermal comfort evaluation

Results show that increase of supply flow rate cause decrease of t_{eq} for MV and hybrid DPV (Figs. 3 and 4). For MV the most intensive cooling was observed for hands, and forearms arms because these body parts were directly exposed to the cool indoor air. Facial region and forehead were also exposed directly to the cool indoor air, but cooling was lesser and temperature difference greater than 1 °C was observed compared to other exposed body parts (Fig. 3). This can be attributed to the convective boundary layer (CBL) generated around heated body. CBL becomes thicker as it rises due to the additional heat flux from the body surfaces and for seated posture due to the interaction of CBL generated around body and legs. CBL generated in the seated posture acts like a layer of thermal insulation from the cool surrounding air in the facial region. On the other hand, forearms and hands are directly exposed to the cool surrounding air and have higher convective heat exchange with the surrounding compared to the facial region.

Hybrid DPV results show that facial region was cooled more intensively than other body parts due to two air jets from DPV (Fig. 3). DPV jets are able to blow-off CBL in the facial region. Increased air velocity and decreased air temperature in the facial region compared to MV case, increased convective heat exchange and resulted in lower t_{eq}. Results also show that increase of the supply flow rate of background MV system cause decrease of t_{eq} in the facial region. In hybrid DPV system supply flow rate increase of the background MV causes more intensive convective heat exchange reducing t_{eq}.

Changes of PPD with the increase of supply flow rate are shown in Fig. 4. Up to 6 ACH, MV and hybrid DPV system have very similar trend, but further increase of supply flow rate cause increase of PPD for hybrid DPV due to overcooling achieved with joint action of DPV jet and increase air velocity of the background MV system.

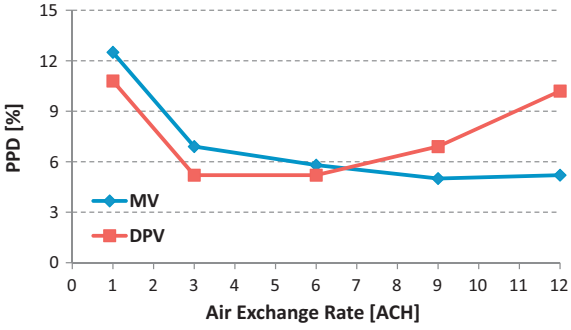

Fig. 4. PPD for various air exchange rates for MV and DPV.

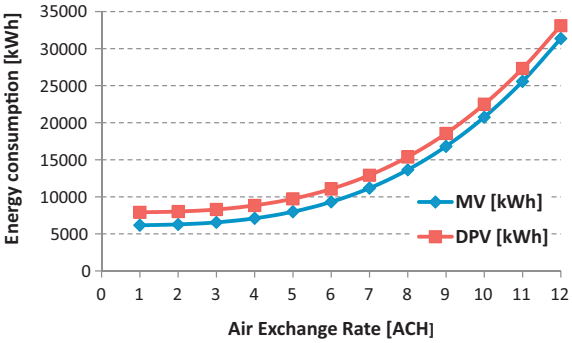

Fig. 5. Total energy consumption for MV and DPV.

3.2. Energy consumption

Energy consumption of the FEC for various supply flow rates is shown in Fig. 5. Energy consumption for 0 ACH would represent a theoretical case in which cooling is achieved with no air supply. Results show that DPV consumes more energy than MV at every supply flow rate. These differences are related to the transport energy, because hybrid DPV required additional ductwork that separately supplies outdoor air from the dedicated AHU.

3.3. Airborne infection risk

Three different regions can be distinguished on infection risk curves. The first region contains very sharp decrease of the airborne infection risks when supply flow rate was increased from 1 ACH to 3 ACH (Fig. 6). For example for the hybrid DPV Flu the second region can be observed when supply flow rate was increased from 3 ACH to 6 ACH because while airborne infection risk was decreased the gradient of change was lower compared to first region. Increase of the supply flow rates beyond 6 ACH reduces airborne infection risk marginally compared to the previous two regions and represents the third region of the curve hybrid DPV Flu curve. Cough droplet dispersion was influenced by the supply flow rate increase which influenced exposure and further determined airborne infection risk. Initially, enhanced dispersion was able to reduce exposure very rapidly, but further increase of supply flow rate had lesser impact on exposure reduction, and beyond 6 ACH impact was significantly reduced.

3.4. Multi-criteria optimization

In this study, five objectives have been included in the multi-objective framework. These are

- power consumption,

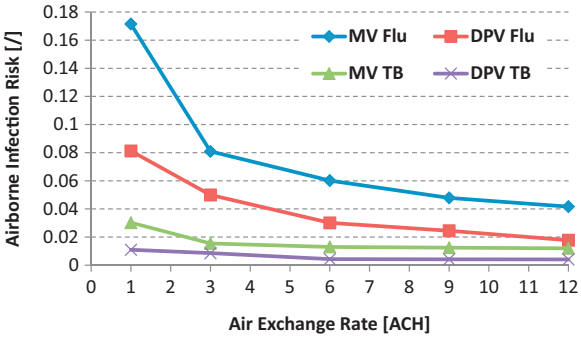

Fig. 6. Airborne infection risk for influenza (denoted as flu on the diagram) and tuberculosis (denoted as TB on the diagram).

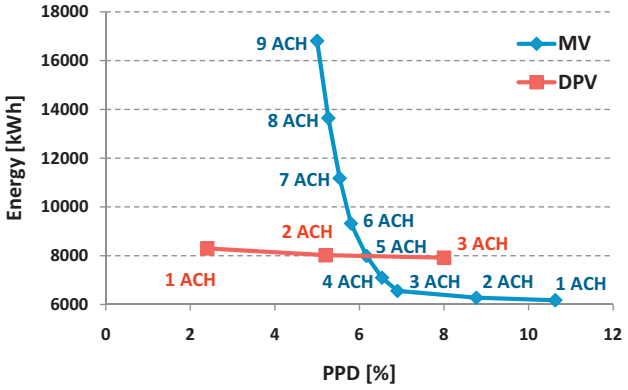

Fig. 7. Pareto front for the objectives power and PPD.

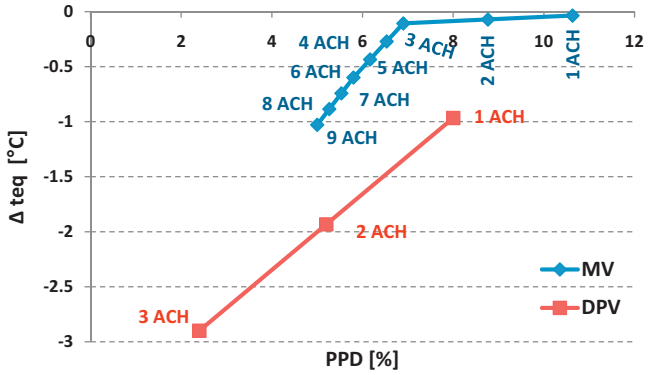

Fig. 8. Overall thermal comfort (PPD) versus Δt_{eq} for MV and hybrid DPV.

- PPD,
- influenza infection risk,
- TB infection risk, and
- Δt_{eq}.

The interactions between these objectives are discussed in this section. The decision variable is the air exchange rate (ACH). The goal is to select the optimal ACH that makes reasonable trade-offs among all the objectives.

The Pareto Fronts for the objectives Energy Consumption and PPD are shown in Fig. 6. PPD increases when Power is minimized through reduction in the air exchange rate (ACH). The Pareto Front represents the trade-off between the two objectives. One objective cannot be improved without sacrificing the other objective. The area below the curve represents infeasible region (where no solutions are possible). The area above the curve represents inefficient region where improvements in both objectives are possible simultaneously. Points corresponding to ACH above 9 are not on the Pareto Front for MV since they result in higher energy consumption and higher PPD. Similarly, ACH above 6 are not on the Pareto curve for DPV. These points are filtered out because they cause simultaneous increase in energy consumption and PPD values. Thus the Pareto front helps to narrow down the selection to a smaller set of solutions. However, it offers no support for selecting the best solution.

It should be noted that all the points plotted on the curves in Fig. 7 are feasible, meaning that they do not violate any technical constraints. The ACH value of 3 for the HVAC system used in FEC is able to fulfill the cooling requirements to maintain setpoint indoor air temperature by supplying air with temperature that will not generate cold zones which may act as possible zone of discomfort for the occupants. However, in a large commercial unit depending on design parameters like thermal insulation of walls, the area of glazing, the number of occupants present, and the thermal load from other devices, this might not be feasible. In that case, this point will not appear on the Pareto front and will not be considered for the selection of the optimal solution.

The value of Δt_{eq} versus PPD for Pareto optimal solutions are plotted in Fig. 8. The value of Δt_{eq} tends to decrease with the air exchange rate, indicating discomfort due to thermal asymmetry. For moderate values of ACH, Δt_{eq} is small and may not cause significant draft sensation. However, if conventional optimization techniques are used to minimize absolute value of Δt_{eq} for reducing draft sensation, it would result in the selection of 0 ACH which is clearly not acceptable. This shows that the problem has to be necessarily treated as multi-objective optimization and Δt_{eq} has to be used in conjunction with PPD rating for a better evaluation of user comfort.

The trade-off between infection risk and power consumption is shown in Fig. 9. Increasing ACH reduces the infection risk of Influenza and TB, but at the cost of increasing power consumption. It can be seen that after a certain level, the reduction in infection risk is marginal, while the increase in energy is significant. Therefore, the choice of optimal air exchange rate should take into consideration the marginal improvements in the values of these conflicting objectives.

3.5. RR-PARETO2 algorithm

The RR-PARETO2 algorithm requires the sensitivity of objectives and the order (priority) of objectives as input. This section demonstrates that this information can be generated through a rational and scientific procedure.

First of all, the order of objectives depends on the scenario. Two scenarios are considered here.

- Scenario S1: Influenza outbreak or world pandemic (e.g. 2009–2010 H1N1).
- Scenario S2: Local or worldwide energy crisis that causes high energy prices.

In the first scenario, the reduction in infection risk becomes the primary objective. Other objectives become secondary. In second scenario, energy prices are high while there is no spread of airborne transmissible diseases beyond expected level; therefore the power consumption becomes the primary objective.

The sensitivity of objectives can be obtained by examining what might be a significant deviation. For the airborne infection risk, a value of 2% represents a change in probability of getting infected that result in less than one new infected case for the given pool of susceptible. This reasoning is based on the well-established epidemiological concept of basic reproductive number which implies

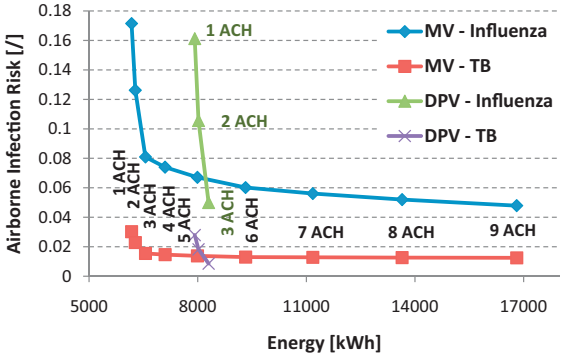

Fig. 9. Infection risk of influenza and TB versus Energy consumption.

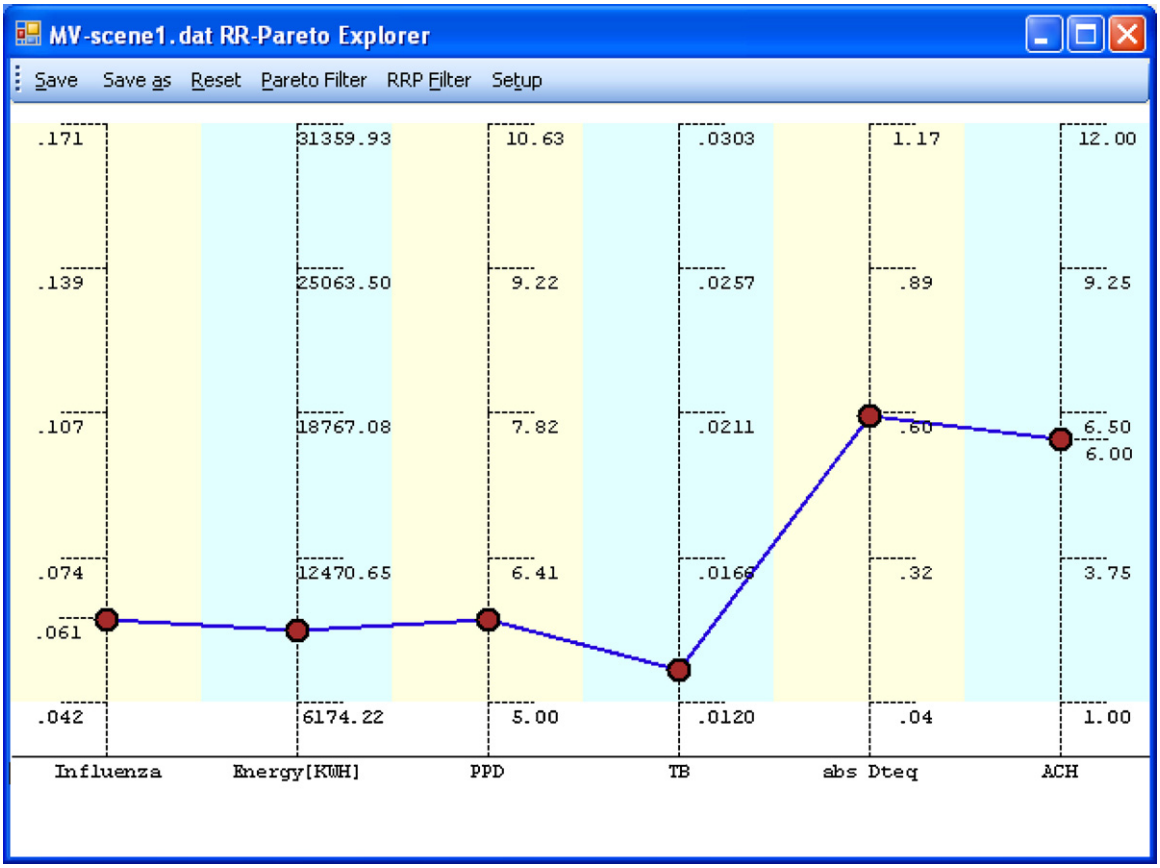

Fig. 10. Optimal solution for Scenario S1 using mixing ventilation.

that infection outbreak will die off in the long run if basic reproductive number is kept below 1 (less than one new infected case) [33]. This is a very strict criterion that can be applied to evaluate protective effectiveness of the air delivery system against airborne infection spread in the indoor environment; therefore it is used as the threshold. In reality, airborne infection can be acquired outside the office building, hence this criterion might not be able to stop office workers from getting infected elsewhere, but it will minimize possibility of airborne transmission inside the indoor environment.

In order to set sensitivity band for energy objective, Singapore building benchmarking scheme called Building Construction Authority Green Mark (BCA-GM) is used as an example [34]. BCA-GM scheme categorize new non-residential buildings into five categories in relation to energy and other green requirements (e.g. water efficiency, sustainable construction, indoor air quality, thermal comfort, etc.). In order to obtain highest level of certification, named Green Mark Platinum, at least 30% of energy savings have to be demonstrated compared to reference model. In order to obtain second highest certification level named Green Mark Gold Plus 25% of energy savings has to be demonstrated compared to the reference model. These two certification levels differ by 5% in energy savings, which could be achieved through operation and design of HVAC system. Hence we have chosen 5% sensitivity bend in this study as an example of optimization performed in Singapore. Sensitivity band could be set in other different ways depending on the priorities and policies of the target organization. For power consumption, a 5% increase is considered to be insignificant in this study taking into account the normal operating costs of a building.

ISO thermal comfort standard for category "A" environments was used to Set bend for thermal comfort. Category "A" environments [35] should have less than 6% of occupants dissatisfied with conditions inside the space. FEC contain 16 workstations, designed to simulate open plan office with 16 occupants. When 6% criteria is applied on the FEC it corresponds to less than 1 occupant to be dissatisfied with thermal conditions. Since thermal comfort model proposed by [30] is based on the whole body thermal sensation, due to concentrated cooling with DPV additional criteria need to be introduced to prevent excessive facial cooling. Manikin based temperature difference (Δt_{eq}) is used as additional condition for DPV and sensitivity band of 1 °C for Δt_{eq} is taken since it is not known to cause significant discomfort and findings from tropical region indicate that subjects perceive air movement to be most acceptable when facial thermal sensation is about "slightly cool" [32].

The order of objectives for the two scenarios are as follows:

- Scenario S1

1. Influenza
2. Power consumption [kWh]
3. PPD
4. TB
5. Δt_{eq} (for DPV)

- Scenario S2

1. Power consumption [kWh]
2. PPD
3. Influenza
4. TB
5. Δt_{eq} (for DPV)

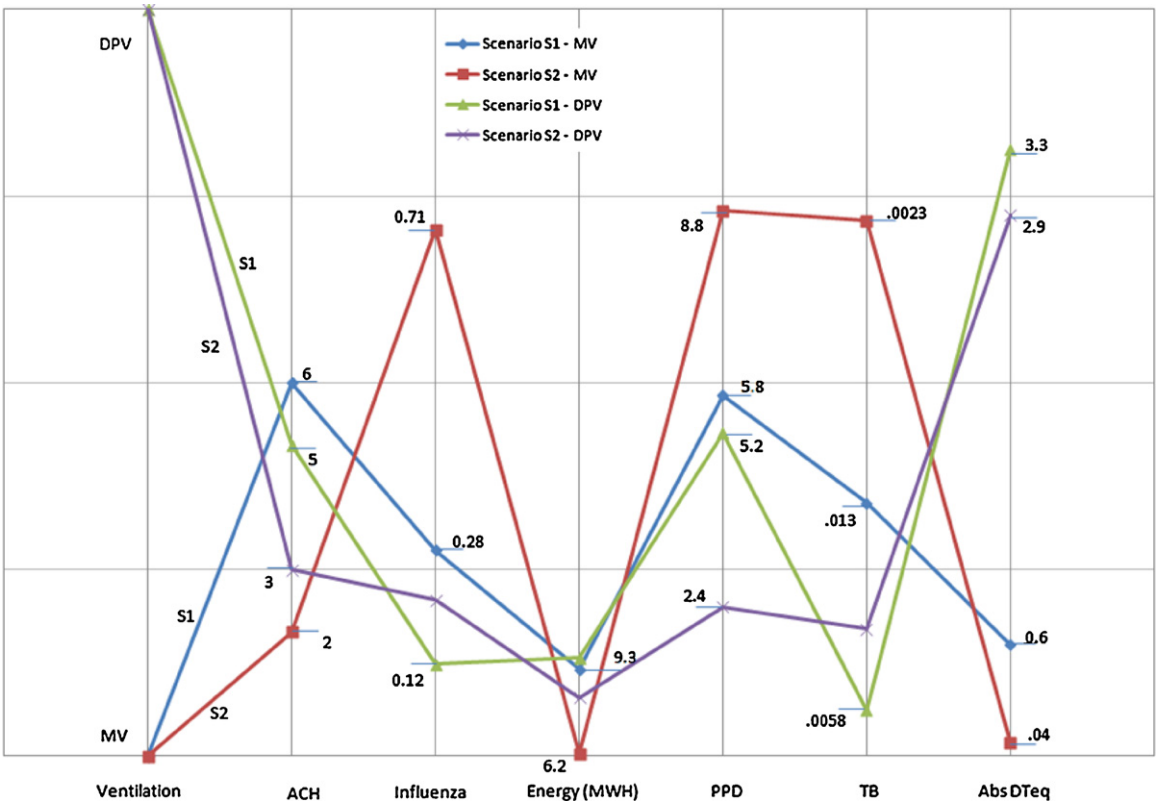

Fig. 11. Optimal solutions for all the cases.

The optimal solution for Scenario S1 using MV is shown in Fig. 10. This involves an ACH of 6 with energy consumption of 9.3 MWH. The optimal solutions for all the cases are summarized in Fig. 11. For Scenario S2, RR-PARETO2 filtering resulted in a solution with an ACH of 2 and energy consumption of 6.3 MWH.

The optimal solutions for hybrid DPV are as follows: The solution for Scenario S1 involves 5 ACH, whereas that for Scenario S2 involves 3 ACH. These correspond to energy consumption of 9.7 and 8.3 MWH, respectively.

For Scenario S1, the optimal solution identified for hybrid DPV has higher power consumption than that for MV. This is because the infection risk for DPV has a lower value than that for MV. If the infection risk for DPV is kept at the same level as that of MV, the optimal solution is 3 ACH with a power consumption of 8.3 MWH which is lower than energy consumption of MV. Comparing this with the power consumption of the optimal solution for MV, there is a savings of 10.7%. That is, for the same level of infection risk, DPV has a lower power consumption compared to MV. Optimization points out solution with much lower primary objective value.

For Scenario S2, hybrid DPV system (Fig. 11) shows higher amount of thermal comfort dissatisfaction compared to MV for low supply flow rates, hence MV performs much better in respect with energy savings for a very low supply flow rates. This result should be taken with caution, because hybrid DPV supply flow rate has been fix, while in reality user would be able to change DPV supply flow rate according to their preference and in that way significantly reduce PPD values for DPV due to microclimate change. This particular behavior was not captured, because it requires test with human subjects while calculations of thermal comfort were performed using BTM. Refinement of thermal comfort results will be attempted in future studies. Table 1 summarises these results.

When solutions involving MV and hybrid DPV were combined and simultaneously considered in the optimization, results for Scenario S1 show that hybrid DPV performs better than MV.

Table 1
Results of RR-PARETO2 filtering.

Scenario	Mode	ACH	Energy (kWh)	Influenza infection risk
S1	MV	6	9323	0.0602
S2	MV	2	6278	0.1262
S1	DPV	5	9737	0.0671
S2	DPV	3	8301	0.0809

RR-PARETO2 algorithm for S1 indicates optimal operation at 5 ACH. This is an important conclusion because it can help designer choose the air delivery system suiting a particular scenario. When S2 is considered, results show the solution is MV with 2 ACH. The energies for all DPV solutions are outside the 5% band. The best solution (MV) has energy consumption of 6174 kWh. The 5% limit of this is around 6480. All the DPV solutions lie outside this band and are eliminated. Sensitivity band of energy has to be increased to at least 45% if DPV is to be selected. If the consideration of prevention of airborne infection risk is of primary concern, such as in the situation of an ongoing or impending pandemic reminiscent of the "Mexican flu" in 2010, then it is likely that facility manager may be professionally obligated to increase the sensitivity band to accommodate the increased priority accorded to mitigating such risks, thereby admitting a solution that has lower infection risk at a higher energy consumption. This underlies the power of this algorithm to dynamically accommodate user articulated priorities and the exploration of alternative solutions.

4. Conclusions

The interactions between the five objectives for the design of a ventilation system have been analysed using the multi-criteria decision-making tool RR-PARETO2. It is shown that the objective

of minimizing power consumption conflicts with other objectives such as thermal comfort and infection risk. The conclusions from this study are the following:

- A multi-objective optimization framework is necessary for selecting the air exchange rate for an HVAC system when criteria such as user comfort, infection risk and energy consumption need to be integrated.
- RR-PARETO2 algorithm shows much potential for identifying solutions that achieve reasonable trade-off among conflicting objectives.
- The optimal solution depends on the scenario under consideration. In the scenario of influenza outbreak, a solution with higher ACH is identified. In the scenario of high energy price, a lower ACH solution is identified.
- For the same level of infection risk, the optimal solution for hybrid DPV has lower power consumption compared to MV. This is very important information since it can lead to strategic choice of the air delivery system. This finding also implies that RR-PARETO2 algorithm can be used as a tool for choosing the air delivery system based on its performance under different scenarios.

In both scenarios that have been studied in this paper, there is a reasonable balance between the values of primary and secondary objectives in the solutions identified by the RR-PARETO2 algorithm. The example demonstrates that the multi-objective framework is valuable for designers in the decision-making process. However, more comprehensive testing using a wider range of problems is necessary for drawing definitive conclusions about the utility of the filtering algorithm. One disadvantage of the algorithm might be the strong dependence on the user defined order of objectives. If the sensitivity band of the most important objective is too narrow, it could result in the selection of the best solution according to this objective. The user has to carefully evaluate the effects of the sensitivity values before making the final selection.

References

[1] J. Huh, M.J. Brandemuehl, Optimization of air-conditioning system operating strategies for hot and humid climates, Energy and Buildings 40 (2008) 1202–1213.
[2] A.P. Wemhoff, Application of optimization techniques on lumped HVAC models for energy conservation, Energy and Buildings 42 (2010) 2445–2451.
[3] J.H. Kämpf, D. Robinson, Optimisation of building form for solar energy utilisation using constrained evolutionary algorithms, Energy and Buildings 42 (2010) 807–814.
[4] L.G. Caldas, L.K. Norford, A design optimization tool based on a genetic algorithm, Automation in Construction 11 (2) (2002) 173–184.
[5] W. Wang, H. Rivard, R. Zmeureanu, An object-oriented framework for simulation-based green building design optimization with genetic algorithms, Advanced Engineering Informatics 19 (1) (2005) 5–23.
[6] Autodesk, Autodesk Ecotect Analysis, 2011, http://www.autodesk.com/ecotect-analysis
[7] M.W. Trosset, I Know It When I See It: Toward a Definition of Direct Search Methods, SIAG/OPT Views-and-News, No. 9, 1997, pp. 7–10 (Fall).
[8] J. Holland, Adaptation in Natural Artificial Systems, University of Michigan Press, 1975.
[9] S. Kirkpatrick, C.D. Gelatt Jr., M.P. Vecchi, Optimization by simulated annealing, Science 220 (4598) (1983) 671–680.
[10] B. Raphael, I.F.C. Smith, A direct stochastic algorithm for global search, Journal of Applied Mathematics and Computation 146 (2–3) (2003) 729–758.
[11] L. Morawska, Droplet fate in indoor environments, or can we prevent the spread of infection? Indoor Air 16 (2006) 335–347.
[12] J.W. Tang, Y. Li, I. Eames, P.K.S. Chan, G.L. Ridgway, Factors involved in the aerosol transmission of infection and control of ventilation in healthcare premises, Journal of Hospital Infection 64 (2006) 100–114.
[13] J.A. Wright, A.L. Heather, F. Raziyeh, Optimization of building thermal design and control by multi-criterion genetic algorithm, Energy and Buildings 34 (2002) 959–972.
[14] N. Djuric, V. Novakovic, J. Holst, Z. Mitrovic, Optimization of energy consumption in buildings with hydronic heating systems considering thermal comfort by use of computer-based tools, Energy and Buildings 39 (2007) 471–477.
[15] M. Hamdy, A.H. Kai Siren, Impact of adaptive thermal comfort criteria on building energy use and cooling equipment size using a multi-objective optimization scheme, Energy and Buildings 43 (2011) 2055–2067.
[16] E.K. Zavadskas, A. Kaklauskas, Z. Turskis, J. Tamosaitiene, An approach to multi-attribute assessment of indoor environment before and after refurbishment of dwellings, Journal of Environmental Engineering and Landscape Management 17 (1) (2009) 5–11, doi:10.3846/1648-6897.2009.17.5-11.
[17] E.K. Zavadskas, A. Kaklauskas, Z. Turskis, J. Tamosaitiene, Selection of the effective dwelling house walls by applying attributes values determined at intervals, Journal of Civil Engineering and Management 14 (2) (2008) 85–93.
[18] E.K. Zavadskas, A. Kaklauskas, Z. Turskis, J. Tamosaitiene, D. Kalibatas, Assessment of the indoor environment of dwelling houses by applying the Copras-G method: Lithuania case study, Environmental Engineering and Management Journal 10 (5) (2011) 637–647.
[19] L. Jelle, J. Arnold, Residential ventilation system optimization using Monte-Carlo and genetic algorithm techniques, IAQ 2010, ASHRAE 2010 Section 6A, 2010, pp 1–10.
[20] Gh. Abdollahi, M. Meratizaman, Multi-objective approach in thermo environomic optimization of a small-scale distributed CCHP system with risk analysis, Energy and Buildings (2010) 3144–3153, doi:10.1016/j.enbuild.2011.08.010.
[21] A. Kusiak, F. Tang, G. Xu, Multi-objective optimization of HVAC system with an evolutionary computation algorithm, Energy 36 (2011) 2440–2449.
[22] B. Raphael, Multi-criteria decision making for collaborative design optimization of buildings, Built Environment Project and Asset Management 1 (2) (2011) 122–136.
[23] B. Raphael, Determination of the optimal positions of window blinds through multi-criteria search, in: Proceedings of the ASCE Workshop on Computing in Civil and Building Engineering, Miami, Florida, 2011, pp. 17–24.
[24] J. Pantelic, G.N. Sze To, K.W. Tham, C.Y.H. Chao, Y.C.M. Khoo, Personalized ventilation as a control measure for airborne transmissible disease spread, Journal of Royal Society Interface 6 (2009) S715–S726.
[25] G.N. Sze To, M.P. Wan, C.Y.H. Chao, F. Wei, S.C.T. Yu, J.K.C. Kwan, A methodology for estimating airborne virus exposures in indoor environments using the spatial distribution of expiratory aerosols and virus viability characteristics, Indoor Air 18 (2008) 425–438.
[26] C.Y.H. Chao, M.P. Wan, A study of the dispersion of expiratory aerosols in unidirectional downward and ceiling-return type air flows using multiphase approach, Indoor Air 16 (2006) 296–312.
[27] S. Zhu, S. Kato, S. Murakami, T. Hayashi, Study on inhalation region by means of CFD analysis and experiment, Building and Environment 40 (2005) 1329–1336.
[28] D. Etheridge, M. Sandberg, Building Ventilation: Theory and Measurement, John Willey & Sons, New York, 1996, pp. 569–696 (Chapter 13).
[29] J. Pantelic, K.W. Tham, Assessment of the ability of different ventilation systems to serve as a control measure against airborne infectious disease transmission using Wells-Riley approach, in: Proceedings of ASHRAE IAQ Conference, Malaysia 2010, Section 7E, 2010, pp. 1–11.
[30] S. Tanabe, E.A. Arens, P.E. Bauman, H. Zhang, T.L. Madsen, Evaluation of thermal environments by using a thermal manikin with controlled skin surface temperature, ASHRAE Transactions 100 (Part I) (1994) 3739–3749.
[31] P.O. Fanger, Thermal Comfort, Danish Technical Press, 1970 (republished by McGraw-Hill, New York, 1973).
[32] N. Gong, K.W. Tham, A.K. Melikov, D.P. Wyon, S.C. Sekhar, K.W. Cheong, The acceptable air velocity range for local air movement in the tropics, International Journal of Heating, Ventilation and Air-Conditioning Engineers (ASHRAE) 12 (4) (2006) 1065–1076.
[33] J. Giesecke, Modern Infectious Disease Epidemiology, Oxford University Press, 2002, pp. 119–133 (Chapter 11).
[34] BCA Green Mark, http://www.bca.gov.sg/greenmark/green_mark_buildings.html
[35] ISO 7730, Ergonomics of the thermal environment – analytical determination and interpretation of thermal comfort using calculation of the PMV and PPD indices and local thermal comfort criteria.